Environmental Science Nano

ROYAL SOCIETY OF CHEMISTRY

PAPER

View Article Online
View Journal | View Issue

Cite this: *Environ. Sci.: Nano*, 2025, 12, 4994

Release of TiO_2 and ZnO nanoparticles from sunscreens into natural waters: detection and discrimination from natural particles using SP ICP-ToF-MS

Maxime Barabash, Houssame-Eddine Ahabchane, Madjid Hadioui and Kevin J. Wilkinson *

From an ecological risk perspective, it is important to differentiate engineered nanoparticles (ENPs) from naturally occurring nanoparticles (NNPs). The aim of this research was to characterize and quantify titanium dioxide and zinc oxide nanoparticles (NPs) that were released from two commercial sunscreens into three aqueous matrices (ultrapure, hard and soft natural waters) after two short term exposures: ~15 min and ~60 min. An inductively coupled plasma time-of-flight mass spectrometer (ICP-ToF-MS) was used to detect elements with mass to charge (m/z) ratios ranging from 26 to 210 amu within single particles (SP). The elemental compositions, mass distributions and isotopic ratios ($^{47}Ti/^{49}Ti$ and $^{66}Zn/^{68}Zn$) of the individual NPs were investigated in order to determine to what extent it was possible to discriminate the natural and engineered NPs. The coupling of an ion-exchange resin to the ICP-ToF-MS resulted in a reduced background signal for zinc, leading to the detection of reasonably small zinc oxide nanoparticles (size detection limit of ~53 nm on the ICP-ToF-MS). For both commercial sunscreens, Zn was primarily released as dissolved forms, with nearly all of the Zn found below the size detection limits or adsorbed to NNPs after 60 minutes. Based upon the SP-ICP-ToF-MS results, the detected NPs in the sunscreens mainly contained single elements, in contrast with the natural NPs. Elemental ratios were helpful to distinguish the ENPs from NPs, but isotopic ratios (Ti or Zn) were not a distinguishing factor for the NPs, in this case. Spearman rank analysis provided an additional index to distinguish the different particle types.

Received 4th May 2025,
Accepted 22nd September 2025

DOI: 10.1039/d5en00444f

rsc.li/es-nano

Environmental significance

This study provides insight into the behaviour and fate of engineered nanoparticles (ENPs) that have been released from commercial sunscreens into natural waters, specifically titanium dioxide (TiO_2) and zinc oxide (ZnO). By employing single particle inductively coupled plasma time-of-flight mass spectrometry, the work examines strategies that can be used to distinguish these anthropogenic particles from naturally occurring nanoparticles (NNPs). Discrimination of the ENPs and NNPs is an essential step that is necessary for accurate environmental monitoring and risk assessment. The study reveals that while ZnO particles tend to dissolve rapidly in natural waters—posing potential risks due to elevated dissolved zinc concentrations—TiO_2 remains predominantly in nanoparticle form. Importantly, the research highlights some of the difficulties in relying solely on isotopic or compositional data for ENP identification by examining single particle characteristics such as particle purity and polydispersity, elemental ratios and isotopic ratios and then applying correlative analysis to the data. This work enhances our understanding of nanoparticle interactions within aquatic environments and underscores the urgent need for refining analytical strategies and regulatory frameworks to address nanoparticle pollution in natural ecosystems.

1. Introduction

Nanomaterials have unique characteristics that make them beneficial in numerous applications. Titanium dioxide (TiO_2) and zinc oxide (ZnO) nanoparticles (NPs) are examples of high production nanomaterials that have been incorporated into a large number of consumer products. For example, sunscreen manufacturers add these NPs to their formulations because of their properties as efficient UV-filters.[1] While a number of studies have demonstrated the potential toxicity of ZnO and TiO_2 engineered nanoparticles (ENPs) to the health of humans[2] or ecosystems,[3–5] it is extremely difficult to quantify their concentrations in natural systems, let alone distinguish them from naturally occurring aquatic colloids (or natural occurring nanoparticles, NNP). The application of sunscreens during swimming activities or their inappropriate disposal during manufacturing are two of the means that these ENPs can find their way into natural waters.[4]

Biophysical environmental chemistry group, University of Montreal, 1375 Ave. Therese-Lavoie-Roux, Montreal, H2V 0B3, Canada.
E-mail: kj.wilkinson@umontreal.ca

Once in the water, sunscreen ENPs can dissolve, agglomerate, sediment and/or be suspended in water columns.[6–9] Their fate will depend on the water chemistry,[10] especially the pH, hardness (or ionic strength),[2] the organic matter content[9,11] and the propensity to interact with components of the natural waters, including the formation of eco-coronas.[12,13] It will also depend upon the formulation of the sunscreen and on the surface properties of the ENP[14–16] including the presence of coatings that tend to improve their dispersion and reduce their agglomeration.[4,15] Some previous studies have characterized the size and shape of ZnO and TiO_2 ENPs from commercial sunscreens in synthetic waters.[5,17] In addition, ZnO and TiO_2 ENPs from sunscreens have been quantified in natural waters,[18,19] generally using electron microscopy[5,18] or single particle inductively coupled plasma mass spectrometry (SP-ICP-MS) based upon quadrupole technology. The SP-ICP-MS techniques are generally very sensitive for measuring low concentrations of small NPs,[20] however, unlike transmission and scanning electron microscopy (TEM and SEM), they are unable to provide information about the particle morphologies.

In spite of their similar compositions, several properties may be useful to differentiate engineered from colloidal particles in natural systems,[7] including particle size distributions and morphologies, elemental or isotopic compositions.[6,21,22] To that end, when SP-ICP-MS is run with a time-of-flight analyser (SP-ICP-ToF-MS),[23] it is possible to detect multiple elements[17] and isotopes[24,25] within a single particle. The major difficulties are related to the technique's relatively high detection limits (making it more difficult to detect small NPs) and the intensive data treatment that is required to process the complex data sets.[20,22,23]

Recent advances in SP-ICP-ToF-MS have enabled high-throughput, multi-elemental characterization of individual particles, providing low-level detection limits and allowing for more confident identification of engineered nanomaterials in complex matrices.[4] For example, Karkee and Gundlach-Graham[22] used SP-ICP-ToF-MS combined with a two-stage hierarchical clustering analysis (HCA) approach to classify and quantify sunscreen-derived TiO_2 and ZnO nanoparticles that were spiked into river water. Their method leveraged the distinctive multi-elemental Ti–Zn signatures of the sunscreen particles, effectively separating them from naturally occurring Fe-, Al-, and Mn-rich particles, and achieving detection for particle number concentrations that were more than 50 times lower than the natural Ti background.[22] Nonetheless, the existing clustering models[26] do not incorporate supervised learning or prior knowledge, potentially limiting classification accuracy in more chemically diverse waters where overlapping particle signatures may occur.[22] These limitations highlight the need for further refinement of classification strategies and validation in real-world environmental contexts—gaps this study aims to address.

The goal of this research was first to collect SP-ICP-ToF-MS data on TiO_2 and ZnO ENP release from two commercial sunscreens into three aqueous matrices. Based upon observed differences among the samples, strategies are then tested in order to distinguish anthropogenically derived particles from natural nanoparticles. Elemental compositions,[27] in addition to mass and isotopic ratio distributions,[24] were examined with the goal of identifying particle characteristics that would best allow the discrimination of Zn- and Ti-containing ENPs from NNPs in natural waters. Discrimination of the natural and engineered NPs would allow us to better follow the fate and determine the risk of the anthropogenic particles in natural waters.

2. Experimental

Analysis of the natural waters

St-Lawrence River (Cartesian coordinates: 45.454009, −73.564012) and Lac-Croche (45.989519, −73.564012) waters (Fig. S1) were sampled using a water sample dipper (SP Bel-Art, USA) immediately followed by a transfer to 500 mL Nalgene bottles. In the following text, waters from the St-Lawrence River and from Lac-Croche waters are referred to as hard and soft waters,[28] respectively (see Table S1 for further information on their compositions). The pH of the waters were measured *in situ* and in the laboratory using an Oakton pH meter following calibration with pH buffers (VWR Chemicals). Water samples were refrigerated in the dark at 4 °C for a maximum of nine days, prior to their use in experiments. On the day of analysis, samples were transferred to graduated polypropylene tubes (Cellstar, Austria), where they were vortexed for 1 min. (Fisher Scientific, Canada), sonicated for 5 min. (5510R-DTH Bransonic® ultrasonic, Danbury, USA) and centrifuged at 3000 × *g* for 5 min. (Heraeus Multifuge 1 S-R, Asheville, USA). The supernatant was carefully sampled then diluted (20–25×) with ultrapure (Milli-Q water, 18.2 MΩ cm at 25 °C, TOC < 2 μg C L^{-1}, Millipore), prior to analysis by SP-ICP-ToF-MS (Nu Instruments Vitesse, United Kingdom).

Release of the sunscreens into the waters

The manufacturers' list of ingredients for the two sunscreens, designated SS1 and SS2, are provided in the SI (Table S2). Based upon the manufacturers' specifications, SS1 contained 24.08% (w/w) ZnO, while SS2 contained 9% (w/w) ZnO and 7% (w/w) TiO_2.

For the particle release experiments, either 28.0–32.0 mg of SS1 or 600.0–650.0 mg of SS2 was applied to the inner walls of a 50 mL polypropylene tube (Greiner Bio-One, Austria), using a cotton tipped applicator (Innovatek, Canada). These quantities were selected on the basis of preliminary experiments in order to have similar numbers of released particles in the waters. SS1 covered approximately 19 cm^2 of the tube, while SS2 covered about 31 cm^2. Sunscreens were applied as uniformly as possible in order to form a thin layer with a thickness of less than 1 mm. A precise mass (~50 g) of each of the three aqueous matrices (ultrapure water, soft water, hard water) was then added to each tube.

Sealed tubes were placed on a circular rotator (Fisher Scientific, Canada; Waltham, USA) where they were rotated at 25 rpm, at room temperature (21 °C), under controlled artificial light. For each water matrix, tubes were collected after 10–20 min and 65–72 min. Water was then transferred into 15 mL polypropylene tubes, where it was again vortexed for 1 min, sonicated for 5 min and centrifuged at 3000 × *g* for 5 min. Based upon Stokes' law calculations, this light centrifugation will only remove large agglomerates that are above the upper measurable sizes of the SP-ICP-ToF-MS. The supernatant was collected and diluted 20–25 times using ultrapure water. Diluted water samples were analysed on the same or following day by SP-ICP-ToF-MS. All tubes were vortexed for an additional 4 min, immediately prior to their analysis. Three experiments were conducted with each sunscreen with waters sampled at different times from the end of May to mid-July 2024.

Digestion and quantitative analysis of the metals in the sunscreens

Sunscreens 1 and 2 were digested to quantify total zinc (SS1 and SS2) and titanium (for SS2). One to three hundred mg of sunscreen were added to 4 mL of a 2 : 1 mixture of sulfuric acid (Omni Trace Ultra, EMP Millipore Corporation; Darmstadt, DE): nitric acid (PlasmaPure Plus, Analytichem; Montreal, CA) in a 20 mL Teflon tube. Samples were digested by microwave (Anton Paar model 20SVT50, Canada) using the following temperature profile: ramp to 150 °C for 15 min, hold at 150 °C for 15 min, ramp to 220 °C for 10 min, hold at 220 °C for 15 min, ramp to 250 °C for 5 min and hold for 15 min. Digestions were performed in triplicate for both sunscreens and standard deviations were provided.

Zinc and titanium concentrations for the digested sunscreens were determined by ICP-MS (NexION 5000, PerkinElmer, Canada) on diluted solutions (2–3 × 10^4 dilution into 2% v/v of a 2 : 1 mixture of H_2SO_4 : HNO_3). Multi-element calibration curves were established by diluting two standards (71A standard, Inorganic Ventures; Ti standard, Analytichem; Montreal, CA) in 2% v/v of 2 : 1 H_2SO_4 : HNO_3. Six concentrations in the range of 2.0 to 40.0 μg L^{-1} were measured from most elements. Quality control standards (QC4, Plasma CAL; QC21, Perkin Elmer; Mississauga, CA) were analyzed following the calibration and after every 12 samples. ^{47}Ti was analyzed in oxygen DRC mode while ^{68}Zn used He KED mode (Table S3). Ionic ^{45}Sc was used as an internal standard. Total metal concentrations for ^{23}Na, ^{24}Mg, ^{27}Al, ^{28}Si, ^{31}P, ^{39}K, ^{43}Ca and ^{56}Fe for the natural waters were also determined by ICP-MS (NexION 5000), except that samples, calibration standards, quality control standards and internal standards were measured in 2% v/v nitric acid. Relative standard deviations for replicate measurements were generally below 2.0%.

Single particle inductively coupled plasma time-of-flight mass spectrometry (SP-ICP-ToF-MS)

One hundred and 400 ng L^{-1} suspensions of PEG carboxyl functionalized ultra uniform gold nanospheres (AUXU50 and AUXU100, NanoComposix, USA) with diameters of 49 and 102.2 nm were used to establish transport efficiencies using the particle size method.[29] In some cases, the waste collection and particle number methods were also used to verify transport efficiencies. Suspensions (200 ng L^{-1}) of citrate functionalized silver nanospheres (AGCN60, NanoXact, USA) with a nominal diameter of 60 nm were used to validate transport efficiency determinations. ICP ionic gold standards (Analytichem, Canada) were used to determine instrument sensitivity using five standards with concentrations ranging from 1.00 to 15.0 μg L^{-1} in 2% v/v hydrochloric acid (Trace Metal Grade, Fisher Chemical). Operating parameters for the ICP-ToF-MS (Vitesse, Nu Instruments, United Kingdom) are provided in Table S4.

ICP-MS standards of titanium (Analytichem, Canada) and silicon (Inorganic Ventures, USA) were added to the multi-element ICP-MS standard 71A (Inorganic ventures). Calibration curves were prepared from five standards in 2% v/v nitric acid (Plasma Pure Plus, Analytichem), with concentrations for most elements ranging from 0.500 to 40.0 μg L^{-1}. Titanium was quantified using ^{47}Ti, whereas zinc was evaluated using ^{66}Zn. ^{47}Ti was used because it has fewer interferences and higher abundance compared to ^{49}Ti. Although ^{48}Ti has an even higher natural abundance (73.72%), we avoided this isotope due to its potential interference with calcium isotopes, particularly in our natural water matrices. The total mass of zinc and titanium was summed from the ICP-ToF-MS data for all of the detected particles. Mass balances were determined by comparing masses detected for the particles with those from the sunscreen digestions and with the manufacturers' stated particle compositions. Measured values of the isotopic ratios of the individual particles were adjusted based upon the isotopic ratios of the ionic standards (*i.e.* the ratios of the sensitivities obtained from the calibration curves for ^{68}Zn, ^{66}Zn or ^{49}Ti, ^{47}Ti; Table S4).

Analysis was performed on a time-of-flight ICP-MS (SP-ICP-ToF-MS, Vitesse, Nu Instruments, UK), equipped with a micro-flow concentric glass nebulizer (0.4 mL min^{-1}), a quartz cyclonic spray chamber (Peltier-cooled to 4 °C) and a quartz injector (1.5 mm internal diameter) with a transport rate of 0.027 mL min^{-1}. Samples were analyzed sequentially starting with the ultrapure water, followed by the soft water and then the hard water. Carryover was monitored and eliminated by rinsing with Milli-Q water between samples.

Preparation and use of the ion-exchange resin for SP-ICP-ToF-MS

Samples were either measured directly by SP-ICP-ToF-MS (without resin) or following their passage over an ion exchange resin. In that case, a PFA column (diameter 12.9 mm, length 64.5 mm; Elemental Scientific) containing the sodium form of a Chelex 100 ion-exchange resin (50–100 mesh, Sigma Life Science, Canada) was placed ahead of the sample introduction on the ICP-ToF-MS.[30,31] Prior to use, the resins were conditioned with 1.5 M nitric acid (Analytichem plasma pure grade) for 20 min at 0.5 mL min^{-1}; ultrapure water (Millipore) for 20 min at 4 mL min^{-1}; 0.1 M sodium hydroxide (ACS, Fisher

Chemical) for 20 min at 0.5 mL min^{-1} and finally with ultrapure water for 20 min at 4 mL min^{-1} using a peristaltic pump (Ecoline, Ismatec). Between subsequent samples, ultrapure water was used to rinse the resin for 4 min at a pump speed of 70 rpm. After the analysis of a maximum of 10 samples, the Chelex-100 resin was rinsed with 1.5 M nitric acid at 0.5 mL min^{-1} for 20 min and then with ultrapure water at 4 mL min^{-1} for 20 min, prior to being sealed for storage.

Treatment of single particle data

Acquired data was processed using Nu Quant Vitesse software (Nu Instruments, UK). Data treatment and analysis parameters, as well as investigated isotopes and their sensitivity are given in the SI (Table S5). TOFVision software developed within our research group[32] was used for further data analysis and the generation of figures. Only particles for which a target element was above detection limits and for which particle numbers were above a detection frequency threshold (>0.2% for the hard water, >1% for ultrapure/soft waters) are presented and discussed. The different detection frequency cutoffs were implemented to maintain equivalent statistical confidence across water matrices with vastly different initial particle abundances.

A Spearman rank correlation analysis was performed to identify monotonic relationships among different element profiles across samples. This non-parametric approach is particularly valuable for elemental composition data, as it is robust with respect to outliers and it doesn't assume linear relationships between variables.[33] The Spearman correlation coefficient between two element vectors A and B is calculated from:

$$\rho = 1 - \frac{6\sum d_i^2}{n(n^2-1)} \quad (1)$$

where d_i represents the difference in ranks between corresponding elemental combinations in the two samples that are being compared, and n is the number of elemental combinations being analyzed. The resulting Spearman correlation coefficient ranges from −1 to 1. Further discussion on the precise approach that was employed is provided in the SI.

3. Results and discussion

Composition of the soft and hard waters

Water samples were collected from an urban hard water and fairly pristine soft water from May to July 2024. Multiple water samples were collected during the sampling period – the soft water was slightly acidic (pH ~6.0) with a dissolved organic carbon (DOC) concentration of ~3.4 mg C L^{-1}, while the hard water was slightly basic (pH ~7.5) with a DOC of ~2.0 mg C L^{-1}. As expected, the hard water had a greater ionic content than the soft water (Table S1). Another striking difference between the two natural waters was the number of particles that were detected by SP-ICP-ToF-MS (Fig. 1). For a similar dilution factor, nearly nine times more particles were detected in the hard water as opposed to the soft water, which was attributed to both the nature of the watershed and the physical differences between the two water bodies (*i.e.* small lake within a forest *vs.* a large river draining a large watershed). When dilutions (20.0 times for soft water and 20.6 times for hard water), analysis time (611 s), ICP-ToF-MS intake rate and transport efficiencies (average 0.4564 μL s^{-1}) were taken into account, total particle number concentrations of 2.6×10^5 particles per mL and 1.8×10^6 particles per mL were determined for the soft and hard waters, respectively.

Based upon both particle numbers and mass concentrations, silicon, manganese, aluminium and iron were the major detected colloidal particles in the two natural waters (Fig. 1). In both natural waters, these elements are likely to be found mainly within oxy-hydroxides and aluminosilicates.[6] Other particles containing iron/manganese and cerium/lanthanum were observed in smaller numbers, consistent with previous reports in other natural waters.[28]

Dissolution of the ZnO NP and improving its detection by ICP-ToF-MS

SP-ICP-ToF-MS measurements were then performed on the two sunscreens (SS1, SS2) that were washed off the inner surfaces of the tubes, during exposure to the three waters: ultrapure water (control), soft water and hard water. In line with the known compositions of the sunscreens, we have focused our analysis on the Zn and Ti containing NP oxides (likely ZnO and TiO_2). In the following analysis, data for two exposure times (~10 min, ~60 min) and three independent experiments (*i.e.* 3 dates) have been combined in order to increase particle numbers and thus statistical significance. Data from the individual exposure times, showing fairly reproducible results from one time to another and from one experiment to another, are provided in (Fig. S2–S5).

When comparing waters with different overall compositions by SP-ICP-ToF-MS, a confounding factor is often the concentration of dissolved metal in the background matrix. For example, zinc oxide nanoparticles are susceptible to dissolution in natural waters.[6,21] An increase in dissolved Zn can make it particularly difficult to detect small Zn-containing NP, as they can be masked by the continuous (background) signal of the dissolved metal. In initial experiments, dissolved Zn was determined by integrating the background signal for the three waters at each of the exposure times. With the exception of SS1 in ultrapure water, dissolved Zn increased as a function of exposure time in all three waters and for both sunscreens (*e.g.* Table S5).

In order to improve the detection of the ZnO NP, a cation-exchange resin (Chelex-100) was placed immediately prior to the sample introduction in order to capture Zn^{2+} ions originating from dissolution of the ZnO NP. This resin has been shown previously to reduce ionic concentrations of the dissolved metals, without significantly reducing particle numbers[30,34] Indeed, in the presence of the resin, the continuous Zn signal decreased and greater numbers of particles were detected (Fig. S6). The resin was able to reduce the dissolved zinc concentration from as high as 2.3 mg L^{-1} (soft water; Table S8) to below instrumental detection limits (Table S6). Importantly,

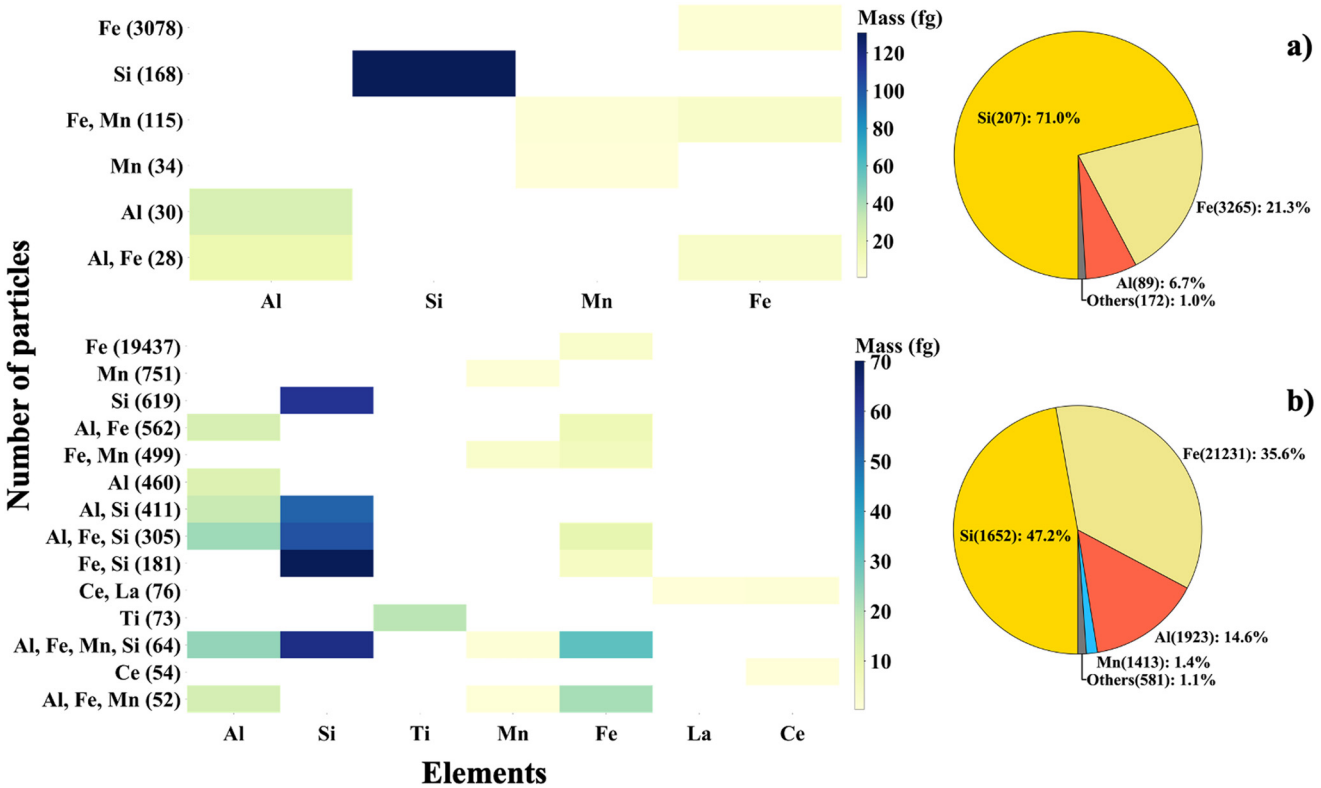

Fig. 1 Elemental heat map of the primary detected particles (left) and overall mass proportions (right) for the aquatic colloids detected in the soft (a) and hard (b) natural waters during the sampling on May 26th, 2024. Note that labels refer to detected particle compositions in the heatmaps, whereas they correspond to overall elemental mass proportions in the pie chart. Results are from a SP-ICP-ToF-MS acquisition of 611 s using a dilution factor of 20.0× for the soft water and 20.6× for the hard water. Numbers in parentheses are particle numbers detected in the diluted samples. Only particles with a detection frequency that was >0.2% of the total particles are presented, the remaining elements are grouped under 'others' in the pie charts. Water samples were passed through a cation-exchange resin prior to analysis.

insignificant numbers of particles (*i.e.* 128 ± 64 particles detected over 210 s or 3.7×10^3 particles per mL) were detected in the rinse waters of the resin, strongly indicating limited or no carryover. On the other hand, the lowering of the dissolved Zn background improved the particle size detection limits in each of the three waters: from 102–130 nm to 53–75 nm.

NP release from the sunscreens into the natural waters

For each of the sunscreens leached into ultrapure water, numerous particle types were detected. Combined data for the two exposure times and three experimental dates for each water matrix are presented in Fig. 2 and 3. For example, for SS1, many of the detected particles were single element Zn particles, representing ~46–56% of the particles in ultrapure water and soft water compared to ~13% of the NP in the hard water. Particles containing both Si and Zn were also detected often (~5% in hardwater and decreasing to ~10% in the softwater and ~4% in the ultrapure water). In fact, silicon represented about 70% of the total mass of the detected particles in SS1 (see Fig. 2). In contrast, the composition of SS2 was more complex with both single element Zn (~2 to 9% in the natural waters and 50% in the ultrapure water), and Ti-containing particles (~31 to 57% in the natural waters and 41% in the ultrapure water) being detected in addition to other particles such as Ti–Zn (~5 to 11%) and Al–Ti (~1% in both natural waters).

While the above proportions were indicative of particle number ratios (Fig. 2a and 3a), particle masses (Fig. 2b and 3b) obtained by SP-ICP-ToF-MS were consistent with both the manufacturer's product description and with the masses obtained by quantitative ICP-MS following digestion of the sunscreens. For example, for SS1, the manufacturer indicated 24.08% of ZnO), in broad agreement with the value of 28 ± 2% determined by acid digestion. For SS2, compositions determined by acid digestion of (6.3 ± 0.2)% (m/m) for TiO_2 and (9.8 ± 0.4)% (m/m) for ZnO were also reasonably consistent with the manufacturers' published values: 7% for TiO_2 and 9% for ZnO. For SS2, silicon NP and less frequently iron NP, were detected in the ultrapure water despite the fact that these elements did not appear on the ingredient list (Table S2).

These experiments were designed, in part, to elucidate the role of the water chemistry on the release of ENP and to provide sufficient databases (two natural waters, two sunscreens, two exposure times) so that it would be possible to distinguish the characteristics of the sunscreen NP (*i.e.* ENP) from the NNP. As expected, the release of the Zn and Ti ENP (presumably ZnO and TiO_2) from the surfaces increased with exposure time (Tables S7 and S8), however, after one hour, the release represented less

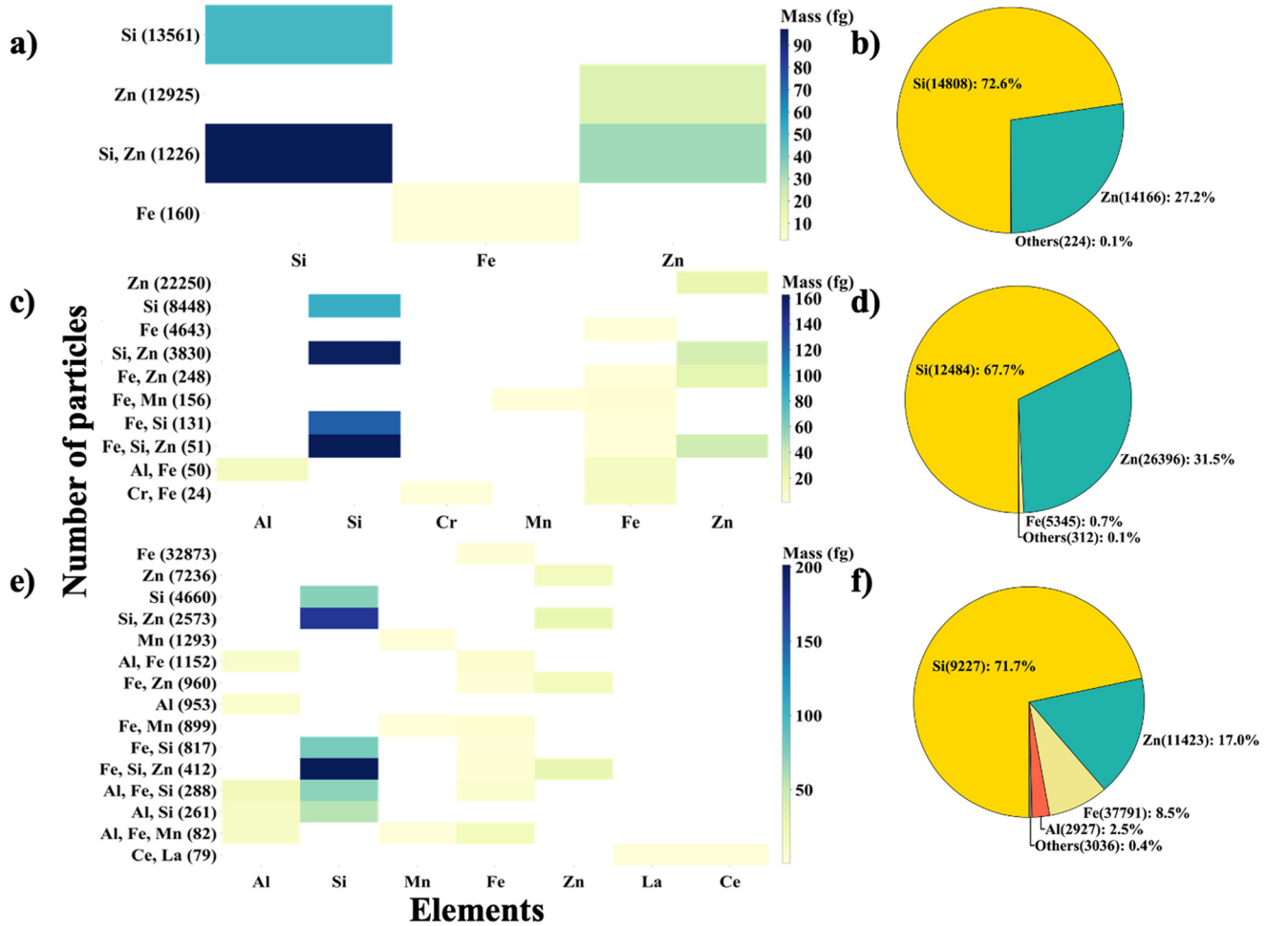

Fig. 2 Measurements of the NP following the release of SS1 into the ultrapure water (a and b); into a natural soft water (c and d) and into a hard water (e and f). Heatmaps (a, c and e) are based upon particle number concentrations (18 minutes of acquisition), whereas pie charts (b, d and f) are based on mass proportions. Note that labels refer to detected particle compositions in the heatmaps, whereas they correspond to overall elemental mass proportions in the pie chart. Data from 3 separate exposure experiments (3 dates) and 2 exposure times have been combined to improve statistics. In the heatmaps, the numbers in parentheses are particle numbers detected in the diluted samples (dilution factors ranging from 19–25). Only particles with detection frequencies >1% are presented here, the remaining elements are grouped under 'others' for the pie charts. All water samples were passed through a cation-exchange resin prior to analysis.

than 1% of the total elemental content of the sunscreens, for all three waters. Furthermore, nearly all of the zinc was measured in dissolved rather than nanoparticulate forms in the natural waters (Fig. S6), which is consistent with the higher solubility of ZnO in natural waters, especially at low pH.[34] This observation was in contrast with the Ti-containing NP in SS2 where titanium release varied from 153 ng per gram of sunscreen at 9 min to 865 ng g^{-1} at 60 min for SS2. Although some Ti NP were measured in the hard water prior to the addition of SS2, the concentrations of the Zn, Zn–Ti and Ti NP also showed substantial increases as a function of exposure time.

What discriminating features can be used to distinguish between engineered NP and natural NP (and colloids) using SP-ICP-ToF-MS?

The time-of-flight analyser is particularly useful for detecting the composition of multi-element particles, however, it remains unclear to what extent SP-ICP-ToF-MS can be used to distinguish between ENP and natural or incidental nanoparticles, especially in chemically heterogeneous and natural waters with numerous polydisperse natural colloids. Given the above data sets of ENP in both ultrapure and natural waters, several strategies for distinguishing ENP and NNP were examined:

1) Under the assumption that ENP are more likely to be mono-elemental,[6] the proportion of single element Ti- and Zn-containing particles were measured in the different natural waters;

2) Particle size distributions were compared, with the hypothesis that ENP are more monodisperse than NNP;

3) Elemental ratios within individual particles were examined with the belief that some elemental ratios would be more characteristic of ENP or NNP;

4) Within individual ENP, certain isotopes may be enriched during the manufacturing process, similar to the observed enrichment of light isotopes by biota in nature.[35]

5) Correlative or clustering strategies using aspects of the above may be useful to distinguish ENP and NNP.

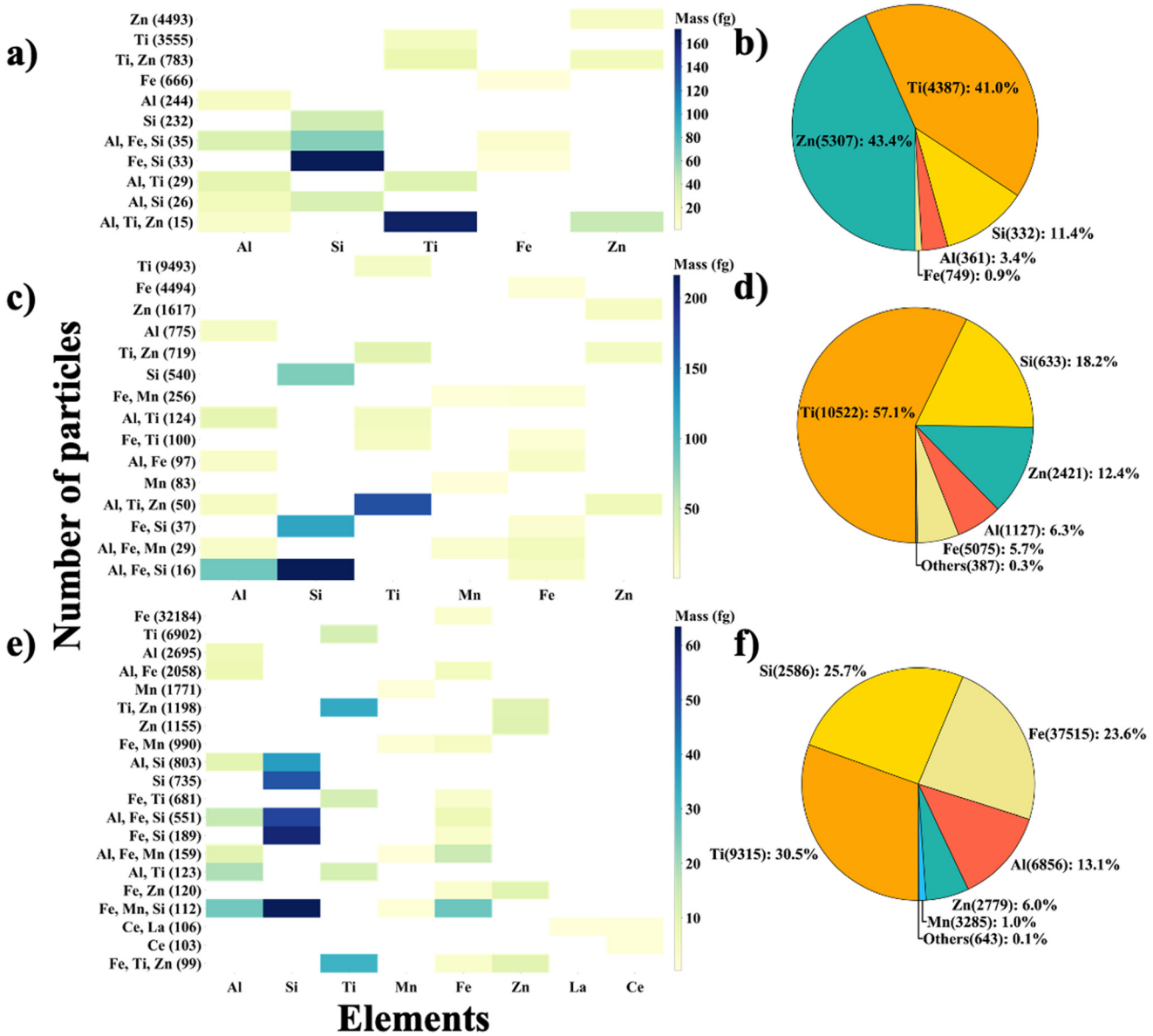

Fig. 3 Measurements of the NP following the release of SS2 into the ultrapure water (a and b), into a natural soft water (c and d) and into a hard water (e and f). Heatmaps (a, c and e) are based upon particle number concentrations (18 minutes of acquisition) whereas pie charts (b, d and f) are based on mass proportions. Note that labels refer to detected particle compositions in the heatmaps, whereas they correspond to overall elemental mass proportions in the pie chart. Data from 3 separate exposure experiments (3 dates) and 2 exposure times have been combined to increase statistical significance. In the heatmaps, the numbers in parentheses are particle numbers detected in the diluted samples (dilution factors ranging from 19–25). Only particles with detection frequencies >1% are presented, the remaining elements are grouped under 'others' for the pie charts. All water samples were passed through a cation-exchange resin prior to analysis.

Natural NP are more likely to be multi-element. For both Zn NP, the proportion of single element particles decreased from the ultrapure water (SS1: 43.4%; SS2: 27.2%; Fig. 2 and 3a) to the soft water (SS1: 12.4%; SS2: 17%; Fig. 2 and 3c) to the hard water (SS1: 6.0%; SS2: 17%; Fig. 2 and 3e). While this observation indicates an increasing proportion of multi-elemental Zn-containing NP in the natural waters, for SS2, the overall Zn NP concentrations also appeared to decrease when comparing the ultrapure (312 ± 180 ng g^{-1}) and the natural waters (soft water: 162 ± 51 ng g^{-1}; hard water: 171 ± 72 ng g^{-1}) (Table S7 for SS1 and Table S8 for SS2). Since no Zn NP were detected in waters that weren't in contact with the sunscreens (Fig. 1), these observations suggest that either fewer particles were being released from the surface of the tube by the natural waters or that particle detection was becoming more difficult (*i.e.* due to increased background in the hard water). However, when an ion-exchange resin was coupled to the SP-ICP-ToF-MS, dissolved Zn in the baseline was negligible and nearly the same in all of the waters (Fig. S6). These observations strongly suggest that it was the chemistry of the natural waters (pH, concentration of Zn ligands) that favoured ZnO dissolution, which would in turn, decrease NP detection.

The formulation of the sunscreen also had a large influence on particle leaching with far fewer Zn NP observed

in the natural waters for SS2 as compared to SS1. Furthermore, in the absence of resin, the concentration of dissolved zinc was 10 to 20 times higher for SS2 compared to SS1, reaching 1928 ± 490 μg L^{-1} in the ultrapure water, 2351 ± 489 μg L^{-1} in the soft water and 1325 ± 357 μg L^{-1} in the hard water after one hour of exposure (Table S5). In addition, for SS2, there was a shift in abundance of the single element zinc particles when comparing the ultrapure water to the natural waters. For example, single element Zn particles represented ~10% of all of the particles containing zinc or titanium (Fig. 4) in the natural waters, while the proportion of single element Zn particles was around ~50% in ultrapure water. Since dissolved Zn concentrations did not change significantly (Table S5) among the different waters, we hypothesize that following the dissolution of the ZnO NP in SS2, Zn^{2+} was adsorbed to the aquatic colloids and NNP that were present in the natural waters. This explanation is consistent with the observation of fewer Zn NP in the natural waters as compared to the ultrapure water and would explain why both fewer NP and a lower proportion of Zn-containing multielement particles were observed in the ultrapure water as compared to the natural waters. The formation of heteroaggregates between the NP and natural particles is also possible, although it might be accompanied by a shift in the mass distributions (which was not the case, see next section).

In SS2, Ti NP concentrations were lower in the ultrapure water (301 ± 161 ng g^{-1}) as compared to the natural waters (soft water: 865 ± 182 ng g^{-1}; hard water: 865 ± 463 ng g^{-1}). Unlike the Zn NP, numerous Ti NP were measured in the natural waters without added sunscreen, although at ppt concentrations (Table S8). The Ti NP are poorly soluble and indeed, good mass balances were obtained when adding particle numbers in the ultrapure water to those detected in the soft or hard waters that had not been in contact with SS2.

Finally, for SS2, particles containing both titanium and zinc were observed in all of the tested waters, for both the short and long release times (Fig. 3), where they ranged from 5 to 10% of the particle numbers. It is unclear whether these particles were chemically heterogeneous particles containing Ti and Zn, heteroaggregates of ZnO and TiO_2 or resulted from Zn adsorption to TiO_2 NP (as above). Given that similar numbers of the Ti–Zn particles were found in the three matrices, it is most likely that the Ti–Zn NP were an original component of the SS2. Although there is no evidence for increased agglomeration as a function of either ionic strength or the concentration of natural particles, increased

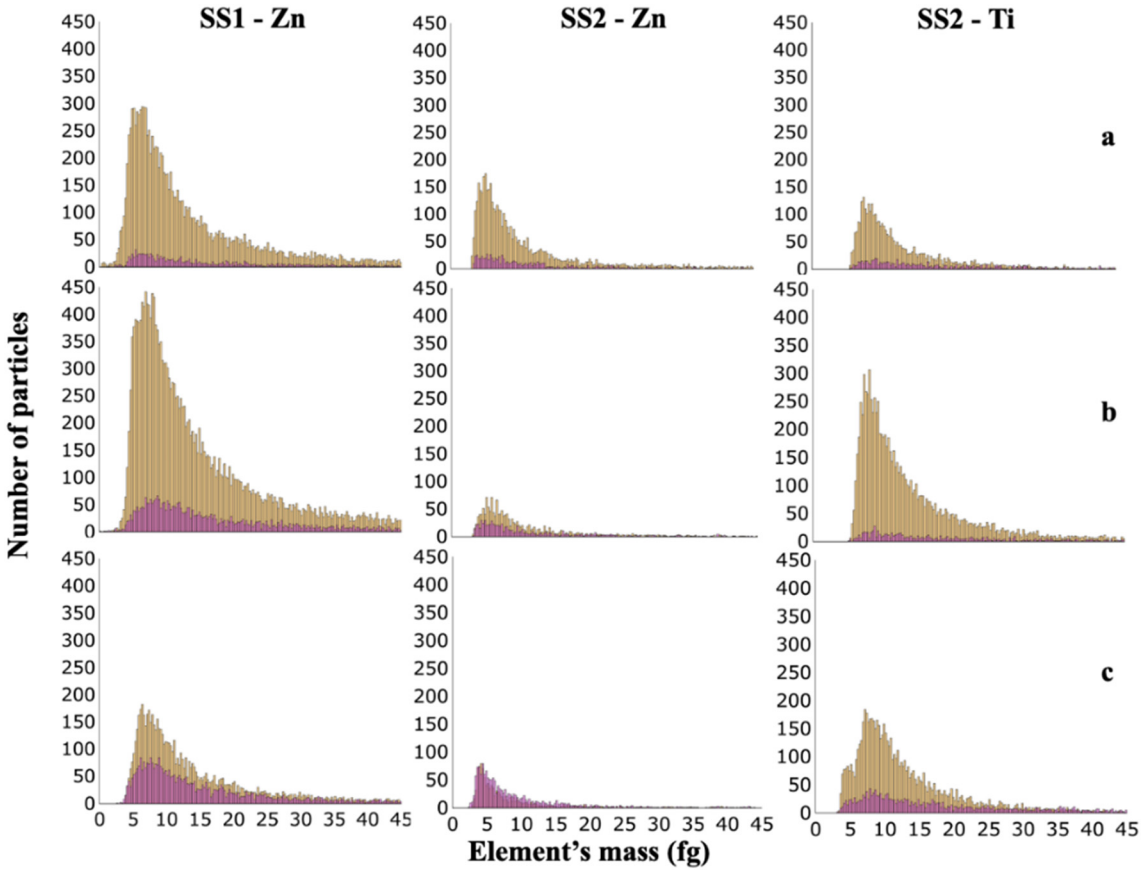

Fig. 4 Mass distribution of titanium and zinc particles released from the two sunscreens (SS1, SS2) in the ultrapure (a), soft (b) and hard (c) waters for combined data representing two exposure times and three experiments. The pink distribution in each figure corresponds to the multi-elemental particles while the orange distribution represents the single element zinc or titanium particles.

Zn adsorption, leading to greater proportions of multi-element particles, may have also been more important in the hard water (see also next section).

Important differences in overall mass distributions of Ti and Zn were not observed. Mass distributions of titanium and zinc NP are presented for the three exposure waters (Fig. 4). For each of the waters, more particles were observed as the exposure time was increased. For each of the NP, mass distributions were similar in a given formulation (vertical direction in Fig. 4). The peak of the distribution was ~6 fg for Zn NP and ~7 fg for Ti NP. Under the (unproven) assumption that the Zn NP in the sunscreen are spherical ZnO with a density of 5.6 g cm^{-3},[36] the radius of the particle peak would correspond to approximately 68 nm. Similarly, if the Ti NP are spherical TiO_2 particles with a density of 4.26 g cm^{-3},[37] 7 fg particles would have a radius of ~87 nm. Furthermore, a similar particle size distribution was observed for the multi-element particles (pink in the figures) as for the single element particles (orange in the figures). On the other hand, the proportion of multi-element particles increased as the waters became more complex (ultrapure to soft to hard waters), which is consistent with the previous observation above that dissolution of the Zn NP was leading to dissolved Zn, which was being adsorbed to the natural particles.

Elemental ratios appear to be useful indicators of particle source

For waters exposed to SS1, particles containing both Si and Zn were detected (Fig. 5). This result is not unexpected given the presence of polydimethylsiloxane (dimethicone) on the ingredients list and its use as lipophilic coating for sunscreen nanoparticles.[14] Such a coating is useful for dispersing the NP in hydrophobic creams.[15] Particles containing silicium and zinc were detected in all exposure waters and for both exposure times. 20–30% of all detected particles containing zinc also contained Si, with a fairly large molar excess of Si. Similar Si/Zn ratios were observed in all three waters (ultrapure, soft- and hard-waters; Fig. 6). This result is in stark contrast with the soft and hard waters that had not been in contact with the sunscreens where only negligible numbers of NP containing both Si and Zn were found.

Fe/Zn ratios were also interesting in that significant numbers of NP containing both elements were observed in the soft- and hard waters following the exposure to the SS1 (Fig. 6). However, in that case, only 2 NP containing both Fe and Zn were observed in the ultrapure water that was in contact with SS1, which is not significant. The absence of Fe–Zn NP in the ultrapure water and their detection in both the soft- and hard waters strongly suggests that they were formed in the natural waters, either through heterocoagulation between Zn and Fe NP or following the adsorption of dissolved Zn on natural Fe NP, again consistent with the mechanisms proposed above for the Zn NP.

Finally, SS2 was shown to generate Fe–Ti containing NP in the three waters. Nonetheless, given the large polydispersity, the large range of Fe/Ti values and the high concentration of Ti-containing NNP (Fig. S7), in this case, it was difficult to distinguish the ENP from the NNP. Indeed for SS2, no elemental ratios were identified that could be used to non-ambiguously distinguish the different kinds of NP.

Finally, note that TiO_2 particles in sunscreens can be coated with an alumina layer[14,15] and thus the Ti/Al ratio has been proposed as another means to distinguish engineered

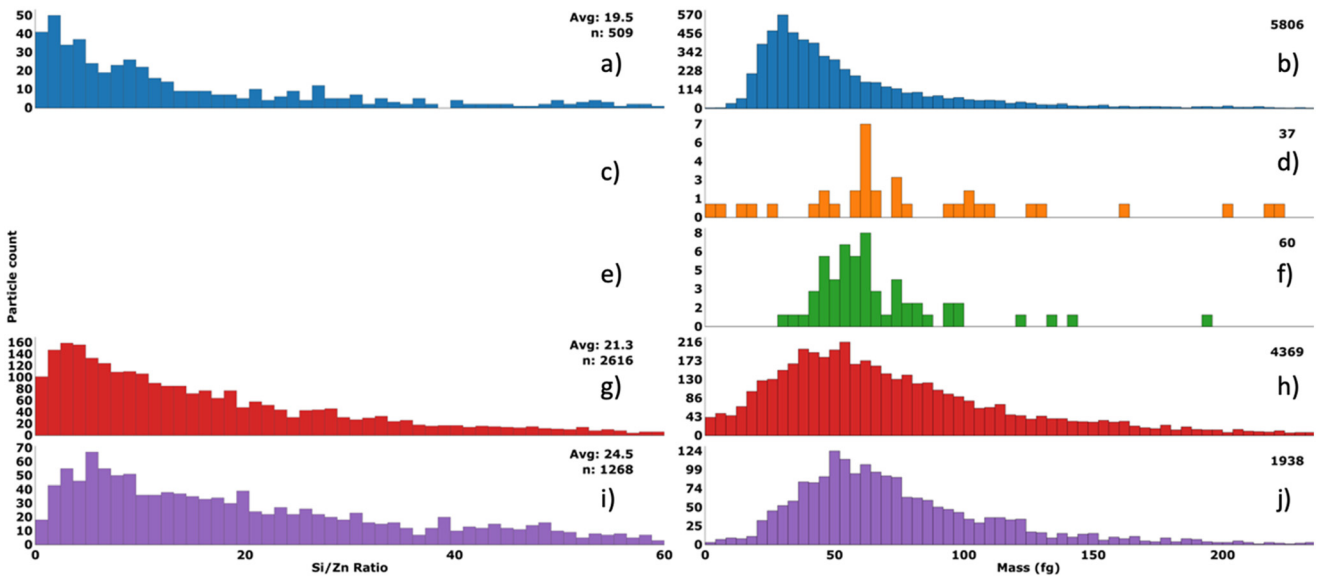

Fig. 5 Si/Zn elemental ratios for the ultrapure water with SS1 (a); the soft (c) and hard waters (e) without SS1; and the soft (g) and hard waters (i) with SS1. Corresponding particle mass distributions for Si are provided in b, d, f, h and j. In both the soft- and hard water without added SS1 (c and e, respectively), no particles containing both Si and Zn were found, although many Si containing particles were found (d: soft water and f: hard water).

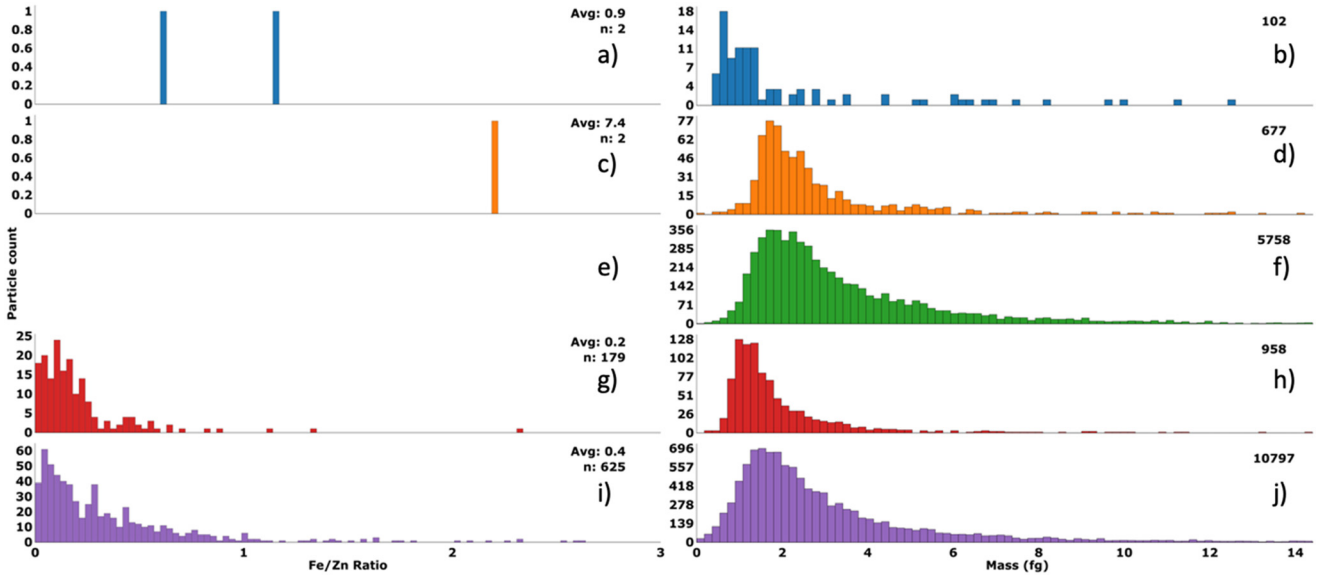

Fig. 6 Fe/Zn elemental ratios for the ultrapure water with SS1 (a); the soft (c) and hard waters (e) without SS1; and the soft (g) and hard waters (i) with SS1 and their corresponding Fe particle mass distributions (b, d, f, h and j). In the soft- and hard waters without added SS1, only negligible numbers of particles containing both Fe and Zn were found (c and e), although large numbers of single element Fe particles were found (soft water: d; hard water: f).

TiO_2 nanoparticles from naturally occurring particles.[18,27] Unfortunately, few particles containing both Ti and Al were found (<30) and a large variability in the Ti/Al ratio was observed, especially for the smallest particles containing less than 50 fg of titanium. By combining data for two exposure times and the three experiments, it was possible to determine a Ti/Al ratio value of <2 for most detected particles originating from SS2 (Fig. S8), however, the large variability both in the Ti/Al ratio and with respect to the particle masses made it difficult to identify a characteristic Ti/Al signature for the ENPs in SS2.

No differences in the isotopic ratios were observed between ENP from the sunscreens and the colloidal particles from the natural waters. Due to the stochastic arrival of

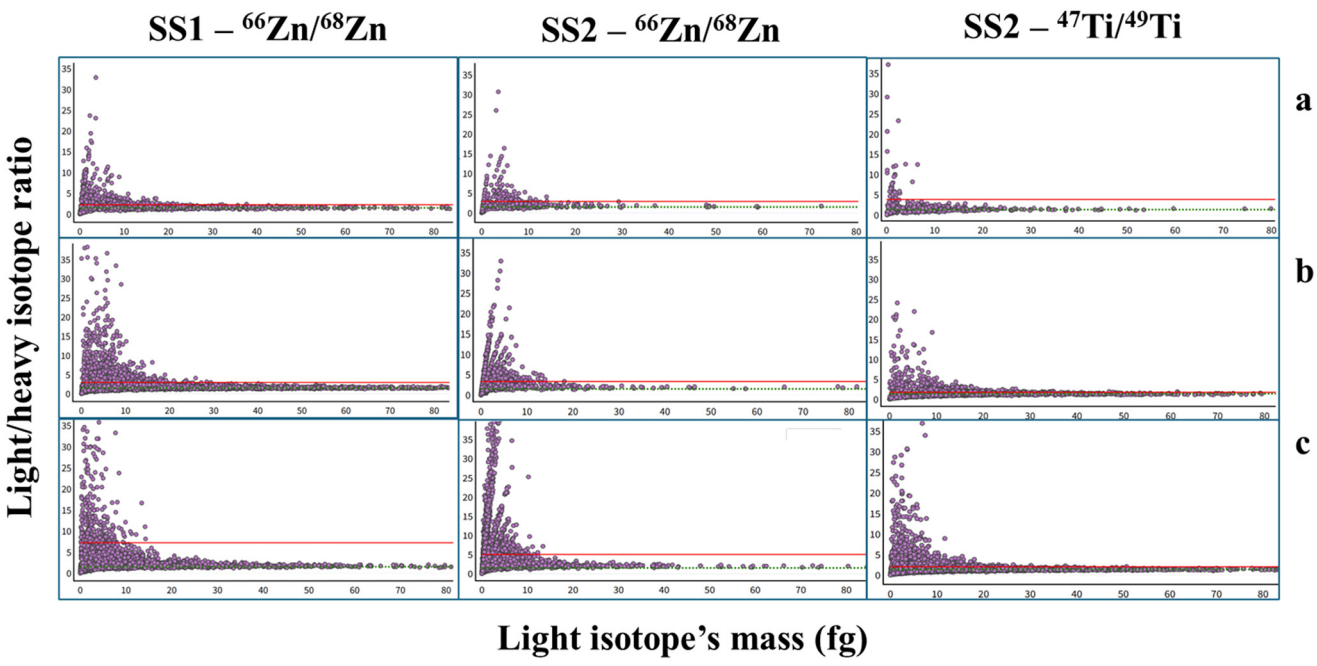

Fig. 7 Isotopic ratios $^{66}Zn/^{68}Zn$ (SS1 and SS2, left) and $^{47}Ti/^{49}Ti$ (SS2, right) as a function of particle mass for the ultrapure (a), soft (b) and hard (c) waters. Results are presented for the experiments of May 28th (SS2, 56–57 min) and June 11th (SS1, 66–69 min). The red line represents the mean isotopic ratio for all of the particles and the dotted green line represents a value that is based on the isotopes' natural abundance.

the ions at the detector and the uncertainty in the gain of the electron multiplier (pulse height distribution), it is difficult to precisely quantify the isotopic ratios of the smallest particles by SP-ICP-ToF-MS.[24] When isotopic ratios for $^{66}Zn/^{68}Zn$ or $^{47}Ti/^{49}Ti$ were corrected under the assumption that the values measured in the ionic standards were representative of natural values, no isotopic enrichment was observed for the larger particles in either SS1 (Zn) or SS2 (Ti). For the most part, isotopic ratios for the particles in the sunscreens (average = red line) were very similar to values expected based upon their natural abundances[38] (dotted green lines) in the ultrapure water (Fig. 7a) and in the soft and hard waters (Fig. 7b and c), although in several cases, the deviation was significant (*e.g.* Fig. 7c, SS1). In all cases, isotopic ratios for the largest particle masses were very similar to those predicted based upon the natural abundances.

Correlative analysis

Many research teams favour the use of cluster analysis to identify similarities and differences among samples acquired using SP-ICP-ToF-MS (*e.g.* ref. 21 and 22). In our experience generally and for these data specifically (*e.g.* Fig. S9), clustering results were highly dependent upon the input parameters (*i.e.* especially the number of clusters selected or the imposed height on the dendrogram). While these inputs can be determined mathematically (*e.g.* silhouette score, elbow method, *etc.*), for the databases studied here (large number of natural particles, few ENP), an 'optimized' low number of suggested clusters (or high height on the dendrogram) led to unsatisfactory results and misidentification of the important particle groups. An alternative strategy (Spearman ranks correlation analysis) was therefore tested in an attempt to provide a strategy that could be used to identify the ENPs in the natural soft and hard waters.

The Spearman correlation analysis employed in this study differs from conventional machine learning approaches in several key aspects. Rather than using cluster-based classification on combined datasets, our method performs pairwise correlations between individual samples and within-sample comparisons simultaneously. This approach allows for direct assessment of relationships between specific

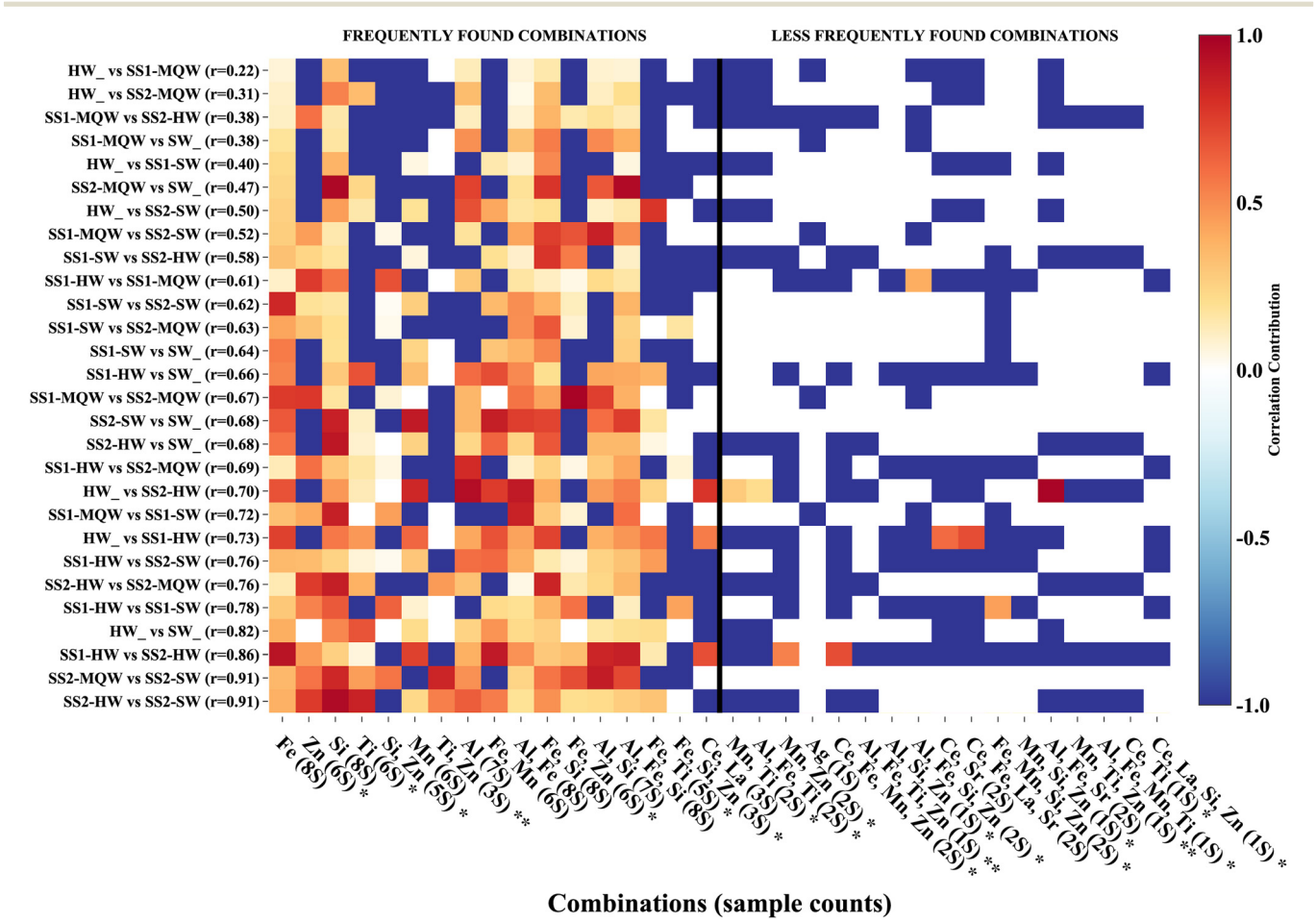

Fig. 8 Spearman correlation analysis to identify the main particle types (*x*-axis) that are useful for the identification of ENPs within a mixture of natural particles. Databases are identified by letters on the *y*-axis (MQW: Milli Q water, SW: soft water, HW: hard water, SS1: sunscreen 1, SS2: sunscreen 2). The asterisks (*) in the figure indicate particles containing Si, Zn or Ti (*i.e.* elements of the ENP).

nanoparticle properties at the individual sample level, while also enabling comparison across the entire dataset. Generally speaking, the correlation-based approach offers advantages in interpretability and direct property relationships, while machine learning methods excel in pattern recognition and classification accuracy.

A Spearman correlation coefficient is generated that ranges from −1 to 1 (Fig. 8), where 1 indicates perfectly similar elemental profiles and −1 represents the case where one sample contains a particular element combination while the other lacks it entirely. Values near 0 indicate that both samples contain limited or negligible amounts of the combination. To account for statistical reliability differences, we implemented a particle count adjustment factor where the similarity score was weighted by the particle counts. For instance, when one sample contains 100 times fewer particles than another, the similarity is reduced by approximately 60%, reflecting lower confidence in the comparison, without entirely discounting compositional similarities that may exist in spite of the count differences. This correction nonetheless prevents an overestimation of the similarities that would be observed when comparing datasets with substantially different particle counts.

The correlation analysis identified a number of important similarities between the sunscreens in the soft and hard waters (SS1, r = 0.76; SS2, r = 0.91) and between the sunscreens in ultrapure water and the natural waters (SS1, r = 0.72 for soft water, r = 0.61 for hard water; SS2, r = 0.91 for soft water, r = 0.76 for hard water) (Fig. 8). There was also a strong correlation observed between the soft and hard waters (r = 0.82). The poorest correlations were observed between the hard water and the sunscreens in ultrapure water (SS1, r = 0.22; SS2, r = 0.31). Note that for a given natural water, the correlation decreased as exposure time increased, reflecting the increased contribution of the sunscreen particles.

In the different binary combinations of the databases, Fig. 8 also shows the factors that were mainly responsible for the strength of the correlations. For example, the Zn, Si and Ti single particles are mainly responsible for the strong correlation seen for SS2 in the soft- and hard waters, whereas the Zn, Si and Zn–Si contributed strongly to the correlation observed between the soft- and hard waters for SS1. In the natural waters, Fe, Si, Ti and Fe–Mn had the largest weight in the positive correlation.

Overall, the correlation analysis was not perfect, but provided a tool that may be of some use for identifying ENP in natural waters, when the database is trained with known particles. When combined with the elemental ratios and especially in the presence of certain specific particle types that are indicative of the ENP, it may be a useful means for separating the ENP from the NNP. Nonetheless, one might also argue that even with all this information on particle compositions, particle sizes and particle concentrations, it is still not a simple task to separate the ENP and NNP. Perhaps this often-overwhelming similarity needs to be better taken into account when evaluating environmental risk.

Conclusion

This research was designed to determine strategies to best distinguish TiO_2 and ZnO ENP from sunscreens from natural Ti- and Zn-nanoparticles and colloids using SP-ICP-ToF-MS. Detection limits of the SP-ICP-ToF-MS were decreased for the ZnO NP by employing a Chelex-100 cation-exchange resin. Even so, based upon the measured mass distributions, the technique is exclusively measuring NP but also a substantial fraction of colloidal particles (both natural and engineered). Although SP-ICP-ToF-MS proved to be a promising analytical technique to study the overall elemental composition of particles, there were numerous similarities among the engineered and natural nanoparticles. Of the strategies examined: particle purity, particle sizes and polydispersity, elemental ratios, isotope ratios and correlative analysis, the elemental ratios and the correlative analysis (based largely upon elemental ratios) appeared to be the most useful indicators to distinguish ENP from NNP. ENP release from the inside of a plastic tube was used as a surrogate for particle release from a surface (skin?) into the natural waters. Water composition clearly influenced both particle numbers and composition of the NP, once released into the water. For the ZnO particles, there was evidence for significant particle dissolution, however, much of the Zn may have been re-adsorbed on the surfaces of natural particles, rather than existing as ionic or dissolved forms in the natural waters. Further studies involving the release of other commercial nanomaterials into natural waters would be helpful to construct a database of common and unique characteristics relative to the ENP, which could then be used with confidence by regulatory organizations to better monitor ENP releases into the environment.

Author contributions

Maxime Barabash developed and conducted the experiments, treated acquired data and arranged the data into figures and tables. Houssame-Eddine Ahabchane constructed Fig. 5–8 and S9 and developed the application TOFVision used to generate the figures and treat the data. Madjid Hadioui helped with the preparation of the cation-exchange resins and assisted with the use of the ICP-ToF-MS. Kevin Wilkinson provided resources for the experiments as well as practical suggestions and contributed to data interpretation and all drafts of the paper.

Conflicts of interest

There are no conflicts to declare.

Data availability

Supplementary information: more information on the natural waters, sunscreens and ICP-ToF-MS operating parameters and detection limits. Additional results, including raw and treated data, heatmaps and clustering analysis are also provided. See DOI: **https://doi.org/10.1039/D5EN00444F**.

Acknowledgements

We acknowledge the financial support of the NSERC Discovery and the NSERC Pure Create network in addition to the Fonds de recherche du Québec – Nature et technologies and Environment and Climate Change Canada.

References

1 V. P. Chavda, D. Acharya, V. Hala, S. Daware and L. K. Vora, Sunscreens: A comprehensive review with the application of nanotechnology, *J. Drug Delivery Sci. Technol.*, 2023, **86**, 104720, DOI: **10.1016/j.jddst.2023.104720**.

2 T. G. Smijs and S. Pavel, Titanium dioxide and zinc oxide nanoparticles in sunscreens: focus on their safety and effectiveness, *Nanotechnol., Sci. Appl.*, 2011, **4**, 95–112, DOI: **10.2147/nsa.S19419**, From NLM.

3 M. Bundschuh, J. Filser, S. Lüderwald, M. S. McKee, G. Metreveli, G. E. Schaumann, R. Schulz and S. Wagner, Nanoparticles in the environment: where do we come from, where do we go to?, *Environ. Sci. Eur.*, 2018, **30**(1), 6, DOI: **10.1186/s12302-018-0132-6**.

4 S. Heilgeist, R. Sekine, O. Sahin and R. A. Stewart, Finding Nano: Challenges Involved in Monitoring the Presence and Fate of Engineered Titanium Dioxide Nanoparticles in Aquatic Environments, *Water*, 2021, **13**(5), 734.

5 A. U. H. Khan, Y. Liu, C. Fang, R. Naidu, H. K. Shon, Z. Rogers and R. Dharmarajan, A comprehensive physicochemical characterization of zinc oxide nanoparticles extracted from sunscreens and wastewaters, *Environ. Adv.*, 2023, **12**, 100381, DOI: **10.1016/j.envadv.2023.100381**.

6 M. Montaño, G. Lowry, F. von der Kammer, J. Blue and J. Ranville, Current status and future direction for examining engineered nanoparticles in natural systems, *Environ. Chem.*, 2014, **11**, 351, DOI: **10.1071/EN14037**.

7 S. Wagner, A. Gondikas, E. Neubauer, T. Hofmann and F. von der Kammer, Spot the Difference: Engineered and Natural Nanoparticles in the Environment—Release, Behavior, and Fate, *Angew. Chem., Int. Ed.*, 2014, **53**(46), 12398–12419, DOI: **10.1002/anie.201405050**.

8 J. Labille and J. Brant, Stability of nanoparticles in water, *Nanomedicine*, 2010, **5**(6), 985–998, DOI: **10.2217/nnm.10.62**, From NLM.

9 M. Arienzo and L. Ferrara, Environmental Fate of Metal Nanoparticles in Estuarine Environments, *Water*, 2022, **14**(8), 1297.

10 C.-P. Tso, C.-M. Zhung, Y.-H. Shih, Y.-M. Tseng, S.-C. Wu and R.-A. Doong, Stability of metal oxide nanoparticles in aqueous solutions, *Water Sci. Technol.*, 2010, **61**(1), 127–133, DOI: **10.2166/wst.2010.787**.

11 R. F. Domingos, N. Tufenkji and K. J. Wilkinson, Aggregation of Titanium Dioxide Nanoparticles: Role of a Fulvic Acid, *Environ. Sci. Technol.*, 2009, **43**(5), 1282–1286, DOI: **10.1021/es8023594**.

12 J. R. Lead, G. E. Batley, P. J. J. Alvarez, M. N. Croteau, R. D. Handy, M. J. McLaughlin, J. D. Judy and K. Schirmer, Nanomaterials in the environment: Behavior, fate, bioavailability, and effects—An updated review, *Environ. Toxicol. Chem.*, 2018, **37**(8), 2029–2063, DOI: **10.1002/etc.4147**, (acccessed 9/2/2025).

13 V. Merdzan, R. F. Domingos, C. E. Monteiro, M. Hadioui and K. J. Wilkinson, The effects of different coatings on zinc oxide nanoparticles and their influence on dissolution and bioaccumulation by the green alga, C. reinhardtii, *Sci. Total Environ.*, 2014, **488**, 316–324, DOI: **10.1016/j.scitotenv.2014.04.094**.

14 J. Labille, R. Catalano, D. Slomberg, S. Motellier, A. Pinsino, P. Hennebert, C. Santaella and V. Bartolomei, Assessing Sunscreen Lifecycle to Minimize Environmental Risk Posed by Nanoparticulate UV-Filters – A Review for Safer-by-Design Products, *Front. Environ. Sci.*, 2020, **8**, DOI: **10.3389/fenvs.2020.00101**.

15 D. L. Slomberg, R. Catalano, V. Bartolomei and J. Labille, Release and fate of nanoparticulate TiO(2) UV filters from sunscreen: Effects of particle coating and formulation type, *Environ. Pollut.*, 2021, **271**, 116263, DOI: **10.1016/j.envpol.2020.116263**, From NLM.

16 R. Huang, Z. Han, C. Ma, H. Liu and X. Huangfu, Stability and mobility of zinc oxide nanoparticles in aquatic environment: Influence of extracellular polymeric substances from cyanobacteria and microalgae, *J. Environ. Chem. Eng.*, 2023, **11**(1), 109069, DOI: **10.1016/j.jece.2022.109069**.

17 B. Bocca, S. Caimi, O. Senofonte, A. Alimonti and F. Petrucci, ICP-MS based methods to characterize nanoparticles of TiO2 and ZnO in sunscreens with focus on regulatory and safety issues, *Sci. Total Environ.*, 2018, **630**, 922–930, DOI: **10.1016/j.scitotenv.2018.02.166**.

18 A. P. Gondikas, F. v. d. Kammer, R. B. Reed, S. Wagner, J. F. Ranville and T. Hofmann, Release of TiO2 Nanoparticles from Sunscreens into Surface Waters: A One-Year Survey at the Old Danube Recreational Lake, *Environ. Sci. Technol.*, 2014, **48**(10), 5415–5422, DOI: **10.1021/es405596y**.

19 L. N. Rand, Y. Bi, A. Poustie, A. J. Bednar, D. J. Hanigan, P. Westerhoff and J. F. Ranville, Quantifying temporal and geographic variation in sunscreen and mineralogic titanium-containing nanoparticles in three recreational rivers, *Sci. Total Environ.*, 2020, **743**, 140845, DOI: **10.1016/j.scitotenv.2020.140845**, From NLM.

20 J. M. Costa-Fernández, M. Menéndez-Miranda, D. Bouzas-Ramos, J. R. Encinar and A. Sanz-Medel, Mass spectrometry for the characterization and quantification of engineered inorganic nanoparticles, *TrAC, Trends Anal. Chem.*, 2016, **84**, 139–148, DOI: **10.1016/j.trac.2016.06.001**.

21 M. Baalousha, J. Wang, M. Erfani and E. Goharian, Elemental fingerprints in natural nanomaterials determined using SP-ICP-TOF-MS and clustering analysis, *Sci. Total Environ.*, 2021, **792**, 148426, DOI: **10.1016/j.scitotenv.2021.148426**.

22 H. Karkee and A. Gundlach-Graham, Two-stage hierarchical clustering for analysis and classification of mineral sunscreen and naturally occurring nanoparticles in river

water using single-particle ICP-TOFMS, *Environ. Sci.: Nano*, 2024, **11**(10), 4162–4173, DOI: **10.1039/D4EN00288A**.

23 Z. Meng, L. Zheng, H. Fang, P. Yang, B. Wang, L. Li, M. Wang and W. Feng, Single Particle Inductively Coupled Plasma Time-of-Flight Mass Spectrometry—A Powerful Tool for the Analysis of Nanoparticles in the Environment, *Processes*, 2023, **11**(4), 1237.

24 S. E. Szakas and A. Gundlach-Graham, Isotopic ratio analysis of individual sub-micron particles via spICP-TOFMS, *J. Anal. At. Spectrom.*, 2024, **39**(7), 1874–1884, DOI: **10.1039/D4JA00121D**.

25 L. Hendriks, R. Brünjes, S. Taskula, J. Kocic, B. Hattendorf, G. Bland, G. Lowry, E. Bolea-Fernandez, F. Vanhaecke and J. Wang, *et al.*, Results of an interlaboratory comparison for characterization of Pt nanoparticles using single-particle ICP-TOFMS, *Nanoscale*, 2023, **15**(26), 11268–11279, DOI: **10.1039/D3NR00435J**.

26 M. Tharaud, L. Schlatt, P. Shaw and M. F. Benedetti, Nanoparticle identification using single particle ICP-ToF-MS acquisition coupled to cluster analysis. From engineered to natural nanoparticles, *J. Anal. At. Spectrom.*, 2022, **37**(10), 2042–2052, DOI: **10.1039/D2JA00116K**.

27 J. Vidmar, T. Zuliani, R. Milačič and J. Ščančar, Following the Occurrence and Origin of Titanium Dioxide Nanoparticles in the Sava River by Single Particle ICP-MS, *Water*, 2022, **14**(6), 959.

28 P. L. Brezonik, W. A. Arnold, P. L. Brezonik and W. A. Arnold, Aqueous Geochemistry I: Inorganic Chemical Composition of Natural Waters, in *Water Chemistry: The Chemical Processes and Composition of Natural and Engineered Aquatic Systems*, Oxford University Press, 2022, pp. 43–82.

29 H. E. Pace, N. J. Rogers, C. Jarolimek, V. A. Coleman, C. P. Higgins and J. F. Ranville, Determining Transport Efficiency for the Purpose of Counting and Sizing Nanoparticles via Single Particle Inductively Coupled Plasma Mass Spectrometry, *Anal. Chem.*, 2011, **83**(24), 9361–9369, DOI: **10.1021/ac201952t**.

30 M. Hadioui, C. Peyrot and K. J. Wilkinson, Improvements to Single Particle ICPMS by the Online Coupling of Ion Exchange Resins, *Anal. Chem.*, 2014, **86**(10), 4668–4674, DOI: **10.1021/ac5004932**.

31 M. Hadioui, V. Merdzan and K. J. Wilkinson, Detection and Characterization of ZnO Nanoparticles in Surface and Waste Waters Using Single Particle ICPMS, *Environ. Sci. Technol.*, 2015, **49**(10), 6141–6148, DOI: **10.1021/acs.est.5b00681**.

32 H.-E. Ahabchane, A. Wu and K. J. Wilkinson, SP-TOF-ICP-MS Analysis 'TOFVision', 2025, **https://github.com/Houssame-EA/TOFVision/tree/main**, (accessed Sept. 11, 2025).

33 C. Reimann, P. Filzmoser, K. Hron, P. Kynčlová and R. G. Garrett, A new method for correlation analysis of compositional (environmental) data – a worked example, *Sci. Total Environ.*, 2017, **607–608**, 965–971, DOI: **10.1016/j.scitotenv.2017.06.063**.

34 L. Fréchette-Viens, M. Hadioui and K. J. Wilkinson, Quantification of ZnO nanoparticles and other Zn containing colloids in natural waters using a high sensitivity single particle ICP-MS, *Talanta*, 2019, **200**, 156–162, DOI: **10.1016/j.talanta.2019.03.041**.

35 F. Ossa Ossa, M.-L. Pons, A. Bekker, A. Hofmann, S. W. Poulton, M. B. Andersen, A. Agangi, D. Gregory, C. Reinke and B. Steinhilber, *et al.*, Zinc enrichment and isotopic fractionation in a marine habitat of the c. 2.1 Ga Francevillian Group: A signature of zinc utilization by eukaryotes?, *Earth Planet. Sci. Lett.*, 2023, **611**, 118147, DOI: **10.1016/j.epsl.2023.118147**.

36 A. Moezzi, A. M. McDonagh and M. B. Cortie, Zinc oxide particles: Synthesis, properties and applications, *Chem. Eng. J.*, 2012, **185–186**, 1–22, DOI: **10.1016/j.cej.2012.01.076**.

37 M. Rajca, R. T. Bray and A. Sokołowska, Granulometric analysis of TiO2 particles in the aspect of membrane filtration, *Desalin. Water Treat.*, 2023, **316**, 583–588, DOI: **10.5004/dwt.2023.30175**.

38 R. D. Vocke, Atomic Weights of the Elements 1997, *Pure Appl. Chem.*, 1999, **71**(8), 1593–1607, DOI: **10.1351/pac199971081593**, (acccessed 2024-12-01).